UNSTEADY AERODYNAMICS OF FLAPPING WINGS

Hiroaki Matsutani
Department of Aeronautics and Astronautics
Graduate School of Engineering, The University of Tokyo

Keywords: *flapping wing, MAV*

Abstract

Birds and insects fly generating thrust by flapping their wings. By emulating this behavior, studies to develop small flying machines are in progress. These machines are called Micro Air Vehicles (MAVs) and are expected to carry various sensors such as visual, acoustic, chemical and/or biological ones.

In this study, two methods are used for the analysis of the flapping wing. First, the vortex ring method is used for the 3-D flapping movement in an inviscid flow. Second, incompressible Navier-Stokes equations and overlapped grids are used for the 2-D heaving movement in a viscous flow.

1 Introduction

Studies of MAVs have become a global issue. Most of the studies are concerned with insect-type MAVs rather than bird-type MAVs. Birds are larger than insects, and it is therefore difficult to replicate the wings of birds for research purposes. The bird-type MAVs, however, have potential advantages such as the ability to fly longer and are less affected by weather conditions [1].

In this study, the level flight of birds is analyzed numerically. First, a simple numerical model of a flapping bird is constructed and analyzed by the vortex ring method [2]. Second, the heaving movement of a two-dimensional flat plate is analyzed by the incompressible Navier-Stokes equations with the overlapped grid systems.

2 3-D Inviscid Flow

2.1 Model of Wing

A lark is selected as a model because of its size and behavior. The weight of the lark W is 0.30N, the span length b is 0.32m, and the wing area S is 0.016m^2. The root chord length c_{root} is assumed to be 0.064m, and thus the model of the wing is formed (Fig. 1). The wing is separated into three parts, that is, the fuselage, the arm and the wrist.

2.2 Model of Flapping

The level flight of a bird consists of the flapping movement and the lead-lag movement.
The flapping movement is regarded as an oscillation of the dihedral angle of the arm and the wrist. The oscillation of the arm is

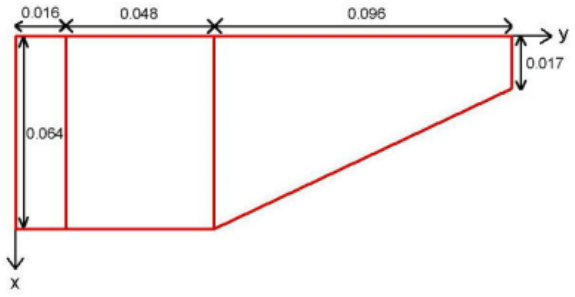

Fig. 1. Lark Wing Model (right half)

$$\gamma_1\,(\text{deg}) = 25\cos(2kt)+20 \qquad (1)$$

and the wrist is

$$\gamma_2\,(\text{deg}) = 35\cos(2kt-0.87)-10 \qquad (2)$$

where k (= $\pi f c_{root}/U$, f: frequency, U: flight speed) is the reduced frequency.

The lead-lag movement is regarded as an oscillation of the distance between the y-axis and the tip of the leading edge, that is

$$l = 0.3c_{root}[\cos(2kt+0.26)+1.0] \qquad (3)$$

The frequency of the flapping is calculated from

$$f(\text{Hz}) = 2.69m^{-0.429} \qquad (4)$$

where m is the mass of the bird (= W/g). So the frequency of the lark f is 12.0Hz from Eq. (4).

The flight speed U can be calculated from

$$mg = 0.3\rho U^2 S \qquad (5)$$

in Ref. [3]. From Eq. (5), the flight speed of the lark U is 7.1m/s when density ρ is 1.225 kg/m^3 and g is 9.81m/s^2, and k becomes 0.34.

2.3 Drag

From the metabolic power, the energy for flight can be approximated by the method in Ref. [4]. The drag is estimated by dividing the flight speed into the energy for flight. The drag curve against U is shown in Fig. 2. At U = 7.1m/s, the drag is 0.049N and the drag coefficient becomes 0.10. The lift coefficient at an angle of attack α = 6deg. is 0.6 from Eq. (5), and these values become the reference.

2.4 Computational Results

The model wing is divided into 12 panels chordwise and 30 panels spanwise, respectively. Each period of the flapping is divided into 40 intervals and the program runs for 80 steps i.e, two flaps. The aerodynamic forces are shown--lift in Fig. 3, induced drag in Fig. 4, thrust in Fig. 5, total drag (thrust subtracted from induced drag) in Fig. 6. The wing and the wake at the 80th step are shown at α = 6deg. in Fig. 7.

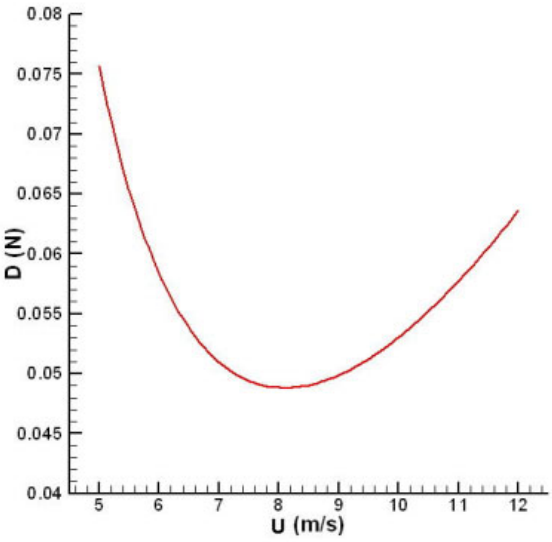

Fig. 2. Drag Curve

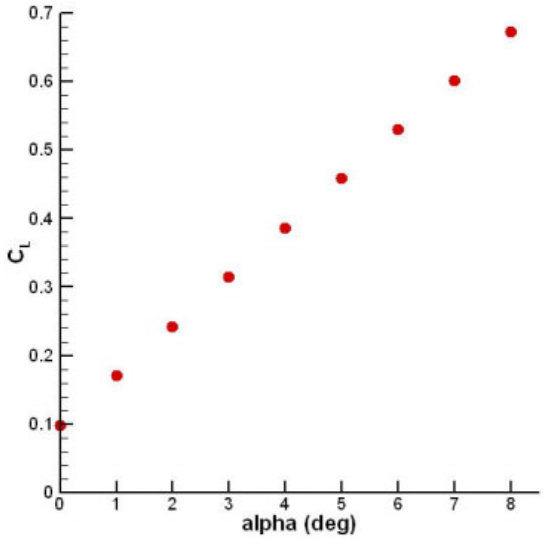

Fig. 3. Lift Coefficient

The lift coefficient C_L is in proportion to the angle of attack, and the lift slope $C_{L\alpha}$ is 4.12/rad. The lift slope of the same but stationary wing is 4.42/rad by the vortex ring method (Fig. 8). These two values are found to be very close. When α is 6deg., the lift coefficient is 0.530 and it is about the same value as that of the reference (0.6). But this calculation does not include the fuselage and tail, and it might realize the reference value when the whole body is included.

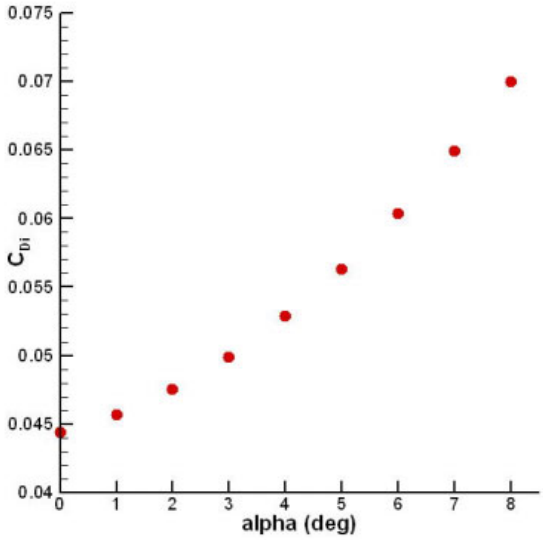

Fig. 4. Induced Drag Coefficient

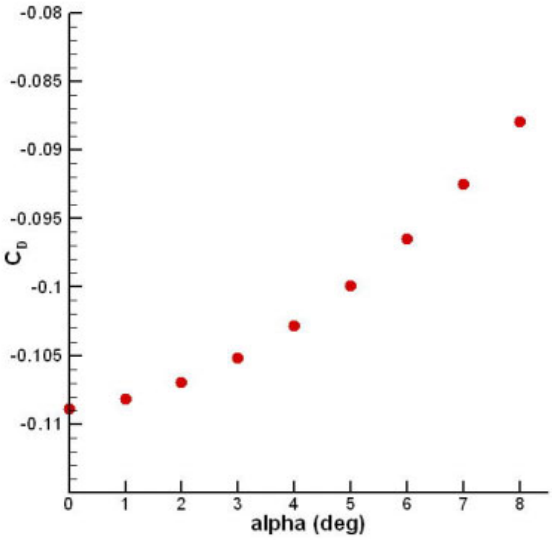

Fig. 6. Total Drag

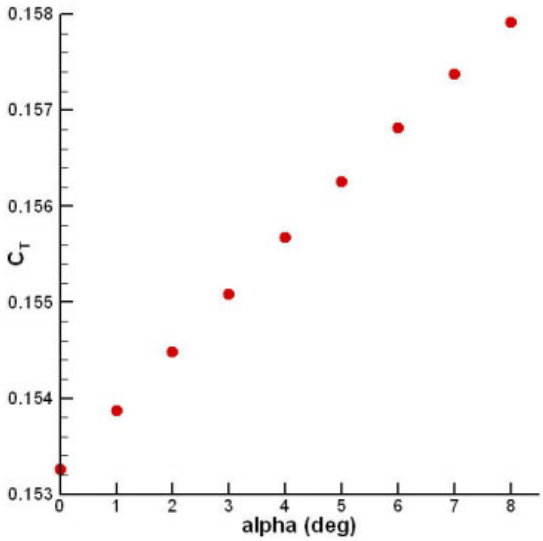

Fig. 5. Thrust Coefficient

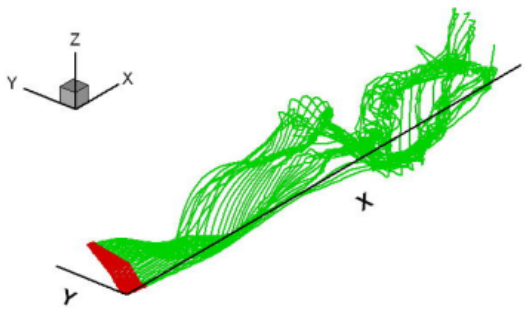

Fig. 7. Wing and Wake（right half）

When an Angle of Attack is 6deg.

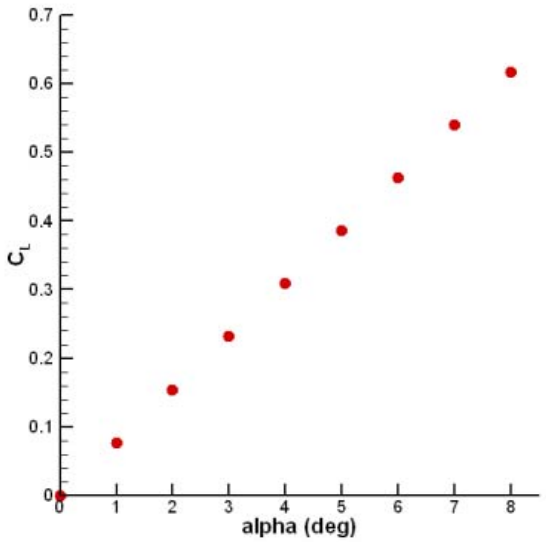

Fig. 8. Lift Coefficient of the Same Fixed Wing

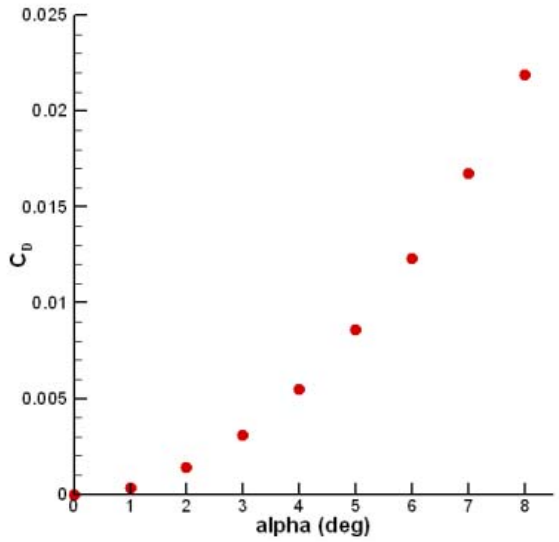

Fig. 9. Drag Coefficient of the Same Fixed Wing

The induced drag coefficient C_{Di} is in proportion to the square of α, that is, of the lift coefficient. This character is the same as a fixed wing. C_{Di} = 0.012 for the same fixed wing (Fig. 9), while C_{Di} = 0.060 for the flapping one at α = 6deg. This is the effect of the near wake and the interaction of the wing-bound vortices. The thrust coefficient C_T is also in proportion to α, but the thrust increase rate is less than that of the induced drag. As a result, the total drag C_D increases against α. The computed thrust coefficient is larger than the reference total drag value 0.10 (includes the viscous effect), so the thrust overcomes the estimated drag.

In Fig. 7, the wake shed from the wrist forms a tube and is turned inward. And the wake shed from the arm also forms a tube and comes outside. Finally, the two tubes makes a larger one. This type of wake is called the continuous vortex gait [1].

3 2-D Viscous Flow

3.1 Navier-Stokes equations

The two-dimensional incompressible Navier-Stokes equations consist of the continuity equation

$$\nabla \cdot \boldsymbol{u} = 0 \qquad (6)$$

and the momentum equation

$$\boldsymbol{u}_t + (\boldsymbol{u} - \boldsymbol{r}_t) \cdot \nabla \boldsymbol{u} = -\nabla p + Re^{-1} \Delta \boldsymbol{u} \qquad (7)$$

with non-dimensional variables (p: pressure, Re: chord Reynolds number). In this study, the x-z plane is used and therefore, components of $\boldsymbol{u}$ are (u, w). The vector $\boldsymbol{r}_t$ represents the velocity of the moving grid.

3.2 Grids

The heaving movement of a flat plate is expressed by using the two grid systems. One is the local grid (Fig. 10) which expresses the neighborhood of the plate and the other is the global grid (Fig. 11) which expresses the whole flow field. The flat plate has a thickness of 2% of the chord length, and its leading and trailing edges are semicircles. The chord length is set at 1.0.

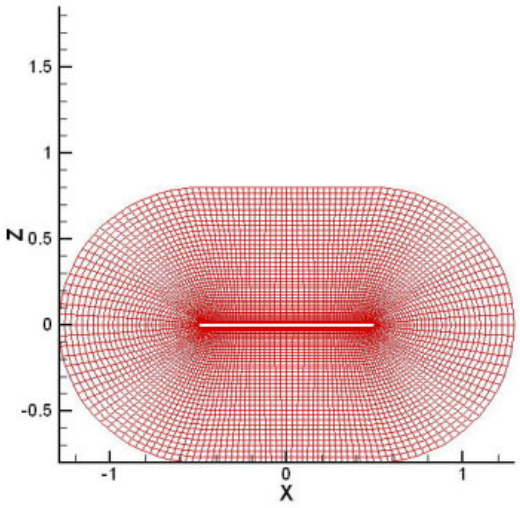

Fig. 10. Local Grid

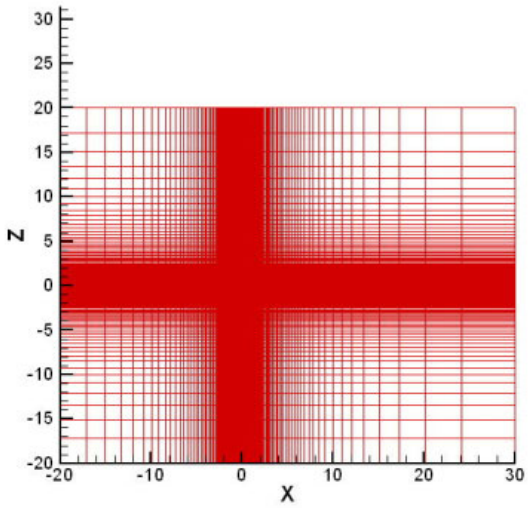

Fig. 11. Global Grid

The local grid moves up and down in the global grid with the oscillation

$$h = h_0 \cos(2kt) \qquad (8)$$

where h_0 is the amplitude, and the origin of the local grid is (0, h) in the global grid. The interaction between the two grids is solved by the method described in Ref. [5].

3.3 Numerical Results

The computational condition is k = 0.34, h_0 = 0.5, a = 6deg. and Re = 1000, and the local grid has 161x41 points and the global one has 121x121 points. Each period is divided into 4000 intervals and the program runs for 8000 steps, i.e, two cycles. The history of the lift, drag and moment about the leading edge coefficients are shown in Fig. 12, Fig. 13 and Fig. 14, respectively. In these figures, 'osc' represents the oscillation h/h_0, the green line represents the force of pressure, the red line represents the force of pressure and friction and the straight lines represent the average of a period. And contour maps of pressure on the local grid are shown in Fig. 15. T represents the period of the heaving movement ($T = \pi/k$).

In the case of potential flow, the shape of the lift coefficient curve becomes sinusoidal, but the result is not smooth in Fig. 12. There are ripples in the curve. Also, the drag and moment coefficients change. These sudden changes occur in the same phases.

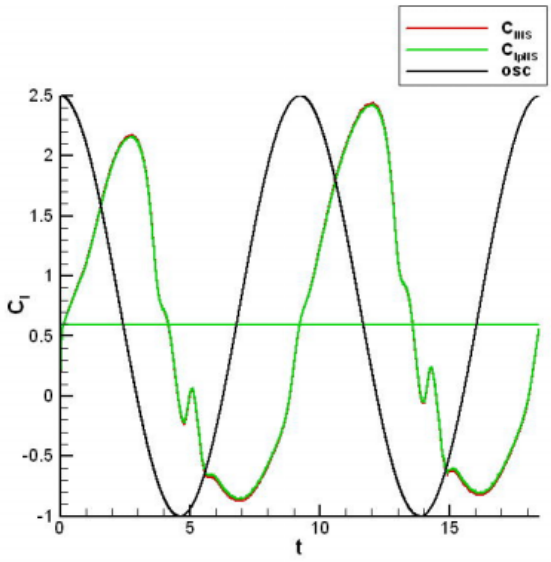

Fig. 12. History of Lift Coefficient

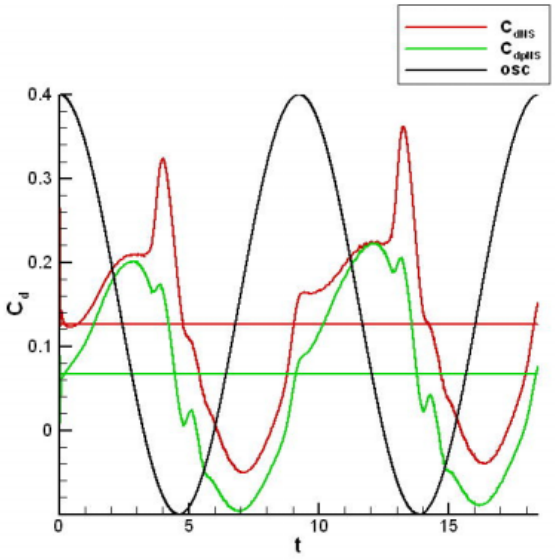

Fig. 13. History of Drag Coefficient

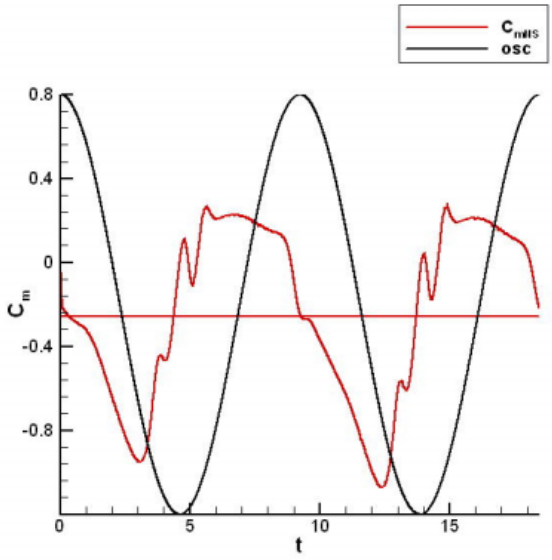

Fig. 14. History of Moment Coefficient

In Fig. 15, vortices can be seen on the upside of the plate. The separation occurs at the leading edge when the downstroke starts (d), vortices move downstream (a) and reach at the trailing edge (b), and a small vortex can be seen at the downside of the trailing edge (c). So, vortices cause the irregular forces.

4 Conclusion

The wing of a lark is modeled numerically by the vortex ring method, and the unsteady aerodynamic forces are calculated. It is found that the lift slope is 4.12 against 4.42 for the fixed wing. The induced drag level is much higher than that of the same stationary wing due to the near wake effect and the interaction of the wing-bound vortices. The wake is well modeled by the present numerical method and the so-called continuous vortex gait is reproduced computationally.

In the two-dimensional viscous flow simulation, we found that although the fundamental frequencies of the unsteady aerodynamic forces are the same as those of the potential flow, there are irregular ripples due to the vortex formation and/or separation. The two overlapped grid systems are effective in the computation.

References

[1] Jeremy M. V. Rayner. Thrust and drag in flying birds: applications to birdlike micro air vehicles. *Progress in Astronautics and Aeronautics*, Vol. 195, pp 217-230, 2001.

[2] Joseph Katz and Allen Plotkin. *Low-speed aerodynamics*. 2nd edition, Cambridge university press, 2001.

[3] Henk Tennekes. *The simple science of flight*. (translation into Japanese by Kenji Takahashi) Soshisha, 1999.

[4] Vance Tucker. Bird metabolism during flight: evaluation of a theory. *Journal of Experimental Biology*, Vol. 58, pp 689-709, 1973.

[5] Kozo Fujii. Unified zonal method based on the fortified solution algorithm. *Journal of Computational Physics*, Vol. 118, pp 92-108, 1995.

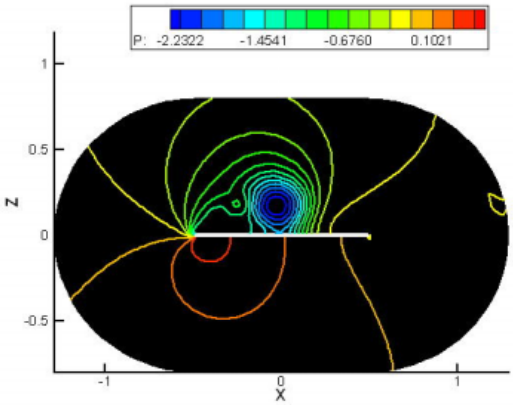

a. t = 11.54 (1.25T)

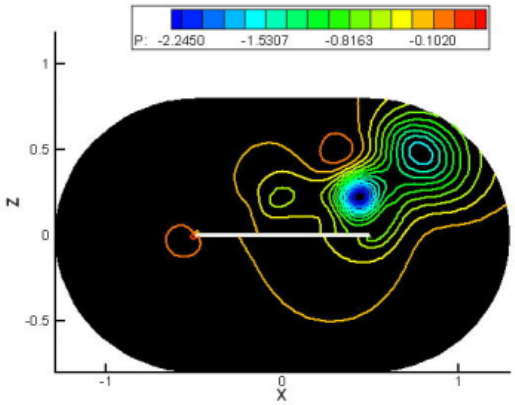

b. t = 13.85 (1.50T)

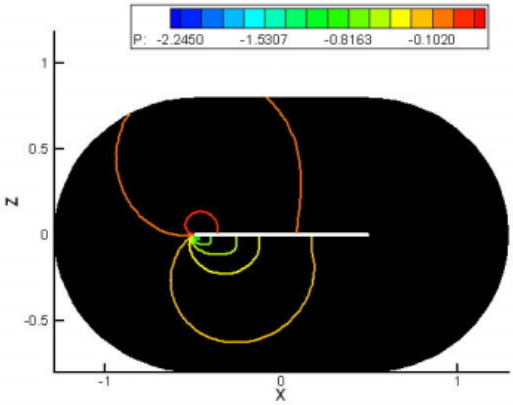

c. t = 16.16 (1.75T)

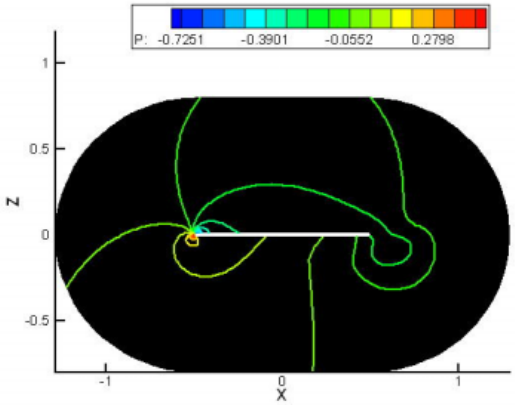

d. t = 18.47 (2.00T)

Fig. 15. Contour Maps of Pressure